Comments on Inorganic Chemistry
Publication details, including instructions for authors and subscription information:
http://www.informaworld.com/smpp/title~content=t713455155

Electron Transfer Modelling of Electrical Dark- and Photoconductivity of Redoxactive Ion Pairs

Horst Kisch[a]
[a] Institut für Anorganische Chemie, Universität Erlangen-Nürnberg, Erlangen, Germany

To cite this Article Kisch, Horst(1994) 'Electron Transfer Modelling of Electrical Dark- and Photoconductivity of Redoxactive Ion Pairs', Comments on Inorganic Chemistry, 16: 3, 113 — 132
To link to this Article: DOI: 10.1080/02603599408035855
URL: http://dx.doi.org/10.1080/02603599408035855

Electron Transfer Modelling of Electrical Dark- and Photoconductivity of Redoxactive Ion Pairs

HORST KISCH
Institut für Anorganische Chemie,
Universität Erlangen–Nürnberg,
Egerlandstr. 1,
D-91058 Erlangen, Germany

Received January 27, 1994

Ion pair charge-transfer (IPCT) complexes consisting of dianionic dithiolene metallates $[ML_2]^{2-}$, M = Ni, Pd, Pt, Cu, Zn, and dicationic 4,4′- and 2,2′-bipyridinium derivatives (A^{2+}) exhibit IPCT bands in the VIS-NIR region of the electronic absorption spectrum. When both components are planar, the solid state structure consists of mixed donor–acceptor stacks while that is not the case when one or both are non-planar. By proper selection of the two components the driving force of electron transfer (ΔG_{12}) from the dianion to the dication is varied from 0.7 to −0.1 eV. It is shown that the Hush relation between optical and thermal electron transfer is fulfilled for a number of thirty-two complexes. The reorganization energy is in the range of 60 kJ·mol^{-1} for the d^8 complexes while it is almost two times larger for the d^{10} zinc compounds. The extent of charge delocalization is typical for outer-sphere complexes as indicated by the parameter α^2 which is in the range of 10^{-4}. Correspondingly, the interaction between the two redox states is rather weak as suggested by the values of 220–360 cm^{-1} calculated for the exchange matrix element. Free activation enthalpies ΔG^* of electron transfer, as calculated within the Hush–Marcus model, amount from 0.15 to 0.73 eV. It is found that the electrical dark conductivity of these composite solids can be quantitatively predicted from ΔG^* in the range from 10^{-10} to 10^{-3} Ω^{-1}cm^{-1} in the case of complexes consisting of planar components (Class I) while in the presence of a nonplanar acceptor or copper as the central metal (Class II) no similar relation is observed. The electrical photoconductivity is wavelength dependent and exhibits a maximum

Comments Inorg. Chem.
1994, Vol. 16, No. 3, pp. 113–132
Reprints available directly from the publisher
Photocopying permitted by license only

in the region of the IPCT band. Laser excitation of the solids produces a transient photovoltage (Dember Voltage) with a half-life of about 20 milliseconds. The results suggest that charge generation occurs by electron transfer and charge migration by a hopping mechanism. When a photoisomerizable olefinic acceptor is employed, the conductivity is ten times larger for the cis-isomer.

Key Words: *charge-transfer complexes, metal dithiolenes, viologens, electron transfer, electrical conductivity, photoconductivity, molecular semiconductors*

1. INTRODUCTION

The rational design of physical properties of solids is a central topic in materials research. Of special interest are optical and electrical properties since light absorption may modify them in such a way that storage of information becomes possible. All that is a typical area of classical solid state chemistry although some recent contributions come from molecular organic chemistry like the nonlinear optical properties of styrylpyridinium compounds[1] or the metallic electrical conductivity of charge-transfer (CT) salts obtained from thetrathiafulvalenes (TTF) and tetracyanochinodimethane (TCNQ)[2] which function as donor D and acceptor A, respectively. The composite nature of CT complexes offers the advantage that relevant molecular properties of the components, like redox potentials which should influence charge-transfer interactions and therefore also conductivity, can be easily varied over a wide range by proper substitution. In the above mentioned CT complexes the specific electrical conductivity (σ) decreases when the oxidizing power of the TCNQ derivative increases while the opposite is observed when tetra-methoxyselenaanthracene (TMSA) is used as the donor. The reason for this behavior may be that the different amount of charge transferred from and to the neutral components D and A can induce different solid state structures and therefore steric effects may overrule the desired electronic influence. This seems not too surprising since the structure of these compounds consists of separated –D–D–D– and –A–A–A– columns which allows only weak *intercolumnar* CT interactions while others, *intracolumnar* of non-CT type, may become more important.[2] Similar results were obtained for metal dithiolenes in different oxidation states[3–6] and for CT complexes of TCNQ with

4,4′-bipyridinium acceptors.[7] Therefore a structure of mixed stacks (−D−A−D−) should be better suited to explore the effect of varying CT interaction on physical properties. In addition, interfering structural changes should be less likely when charged components of planar geometry are employed which retain their planarity in the oxidized and reduced forms. From this background it seemed worthwhile to synthesize light-sensitive ion pair (IP) complexes of the type $\{D^{2-}A^{2+}\}$ wherein both components can undergo reversible electron transfer in the ground state. The complexes investigated are summarized in Fig. 1. They consist of a dianionic

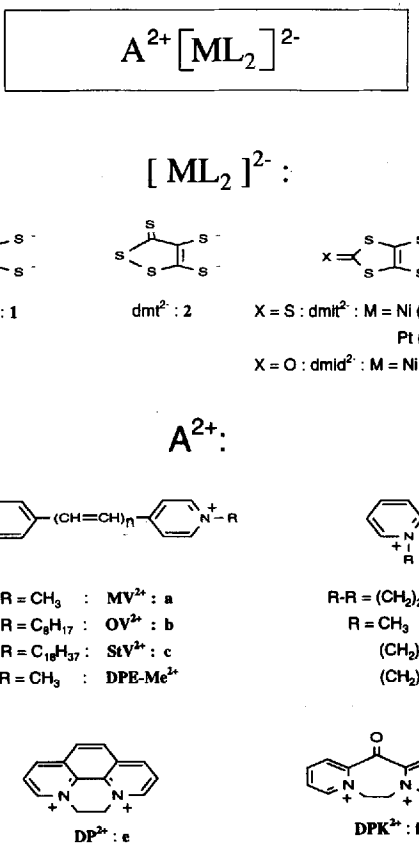

FIGURE 1

metal dithiolene $[ML_2]^{2-}$ and a dicationic 2,2′- or 4,4′-bipyridinium derivative A^{2+}, both of which may have a planar or non-planar geometry. The components were selected in order that the driving force of electron transfer from the donor to the acceptor changes from 0.7 to −0.1 eV. In addition to the d^8-systems Ni(II), Pd(II) and Pt(II), also a few complexes of the d^9 metal atom Cu(II) were investigated. We note that the electrical conductivity of neutral and partially reduced metal dithiolenes was first investigated by Schrauzer[8] and later by Underhill, Cassoux and Kobayashi.[3] In almost all cases the counterions were not redoxactive. The work on mnt-complexes was reviewed recently.[9]

In this review we shall first report on the solid state structure of these ion pair complexes, then discuss the relation between optical and thermal electron transfer on the basis of the Hush–Marcus model, and finally we address the question whether the electrical dark and photoconductivity is significantly influenced by molecular electron transfer properties. In addition we briefly mention how the conductivity is influenced by steric effects like cis-trans isomerization of an ethene-bridged bipyridinium acceptor. Photoinduced electron transfer within these ion pairs has been summarized recently.[10]

2. SYNTHESIS AND STRUCTURES

Methyl viologen salts of halogenometallates were reported more than fifty years ago by Emmert and Lauritzen[11] and were later fully characterized by Williams *et al.*[12,13] $\{MV^{2+}[Ir(mnt)(CO)_2]_2^{2-}\}$[14] and $\{MV(anthracene)\}^{2+}$ were previously synthesized, the latter even in a zeolithe cage,[15] and characterized by X-ray analysis. Inclusion complexes with crown ethers are known also.[16] Very recently the complexes $\{MV^{2+}(eosin)^{2-}\}$ and $\{BV^{2+}[BV^{2+}(eosin)_2^{4-}]^{2-}\}$, BV^{2+} = benzyl viologen, and their X-ray structures were reported.[17] The compounds discussed here are conveniently prepared by metathesis which occurs upon combination of acetone solutions of $(NBu_4)_2[ML_2]$ and $A[PF_6]$ since the products immediately precipitate due to their insolubility.[18–20]

The structure of $MV[Zn(mnt)_2]$ consists of pseudo-columns of tetrahedral $[Zn(mnt)_2]^{2-}$ and non-planar MV^{2+} units (Fig. 2).

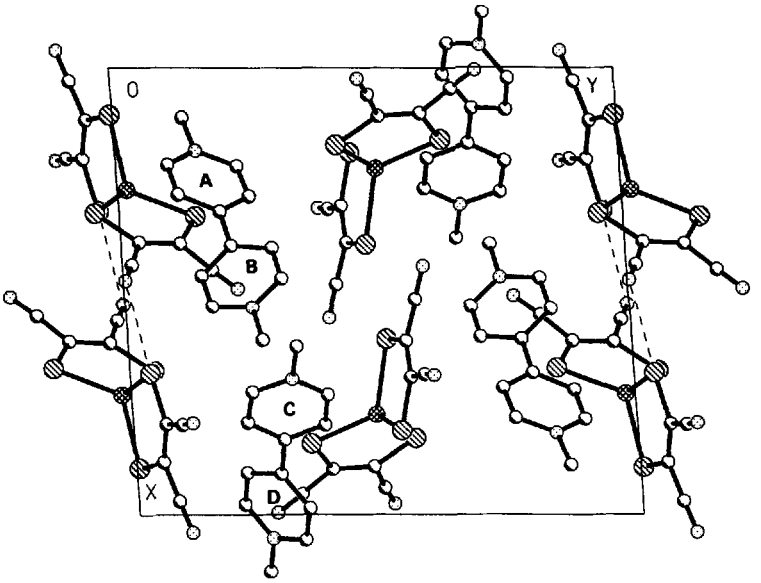

FIGURE 2 Solid state structure of MV[Zn(mnt)$_2$].

Two independent ion pairs are found in the unit cell which differ by the relative donor–acceptor arrangement. In one pair the viologen (A,B) is twisted by 34° around the central C—C bond and the interplanar angles between the pyridinium rings, and two planar halves of $[Zn(mnt)_2]^{2-}$ are 85° and 37°. The other pair has the slightly different angles of 39° (C,D), 85° and 52°, respectively. Short intercolumnar distances occur from the aromatic viologen hydrogen atoms to Zn (320 pm) and S (290 pm), while within the dithiolene zincate pseudocolumns a short contact of 310 pm is observed between the cyano nitrogen and a sulfur atom (Fig. 2, dashed lines).

Changing the geometry of the dithiolene metallate to planar by substituting nickel for zinc induces planarity for the viologen component as indicated by the structure of MV[Ni(mnt)$_2$] which consists of mixed columns (Fig. 3) along the x-axis.[21] The planar ions are arranged face-to-face approximately parallel to each other with an interplanar angle of 5°. The centers of the two components are offset (slipped) by 150 pm. This type of orientation therefore max-

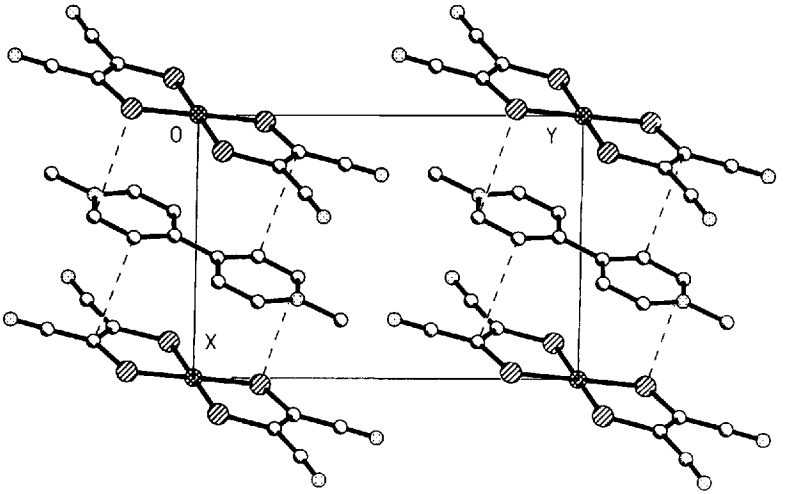

FIGURE 3 Solid state structure of MV[Ni(mnt)$_2$].

imizes attractive charge–charge interaction and minimizes π-π repulsion.[22] The shortest interplanar distances are 360 and 340 pm, values typical for organic CT complexes,[23] and occur between sulfur atoms and the carbon atoms in ortho-position to the viologen nitrogen which are known to carry the highest positive charge,[24] and between a sp^2 carbon atom of the mnt-ligand and the meta-carbon atom of MV^{2+} as indicated by the dashed lines in Fig. 3.

When in the above complex palladium is substituted for nickel, in the resulting ion pair MV[Pd(mnt)$_2$] the basic structural features, including the short interionic contacts, remain the same.[25] This indicates that the solid state structure is not influenced by CT effects since $[Pd(mnt)_2]^{2-}$ is by 0.2 V a poorer donor than the nickel complex.[26]

When MV^{2+} is replaced by the non-planar 2,2′-bipyridinium acceptor BQ^{2+} (Fig. 4), a different structural type is obtained for the resulting BQ[Ni(mnt)$_2$] ion pair.[27] The two pyridinium rings are twisted by 64° and therefore only one of them is oriented face-to-face to one dianion while the second one interacts with another dianion. The angle between the corresponding donor and acceptor planes is 5°. A short interionic contact of 323 pm is found between a pyridinium carbon atom and nitrogen of the cyano group (dashed

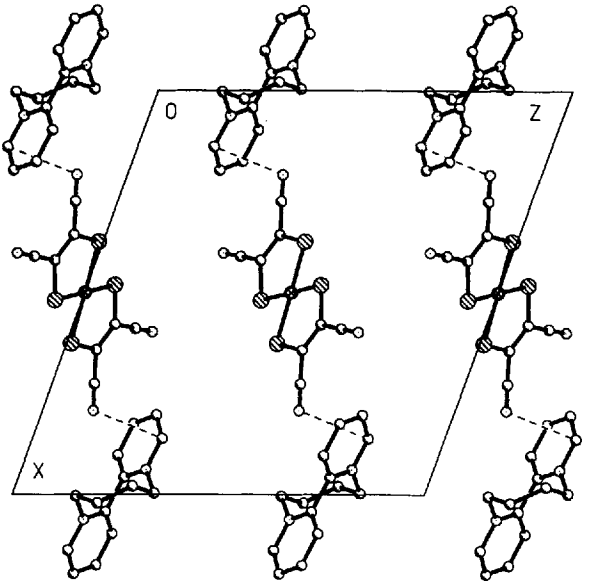

FIGURE 4 Solid state structure of $BQ[Ni(mnt)_2]$.

line in Fig. 4). The structure does not change significantly when in this compound nickel is substituted by cobalt.[28a]

In summary we conclude that tetrahedral d^{10} donors like $[Zn(mnt)_2]^{2-}$ induce a twisted conformation of the acceptor MV^{2+} while the planar $d^{7,8}$ donors $[M(mnt)_2]^{2-}$ also enable a planar geometry of the acceptor[28b] which leads to formation of mixed donor–acceptor stacks. This donor–acceptor arrangement should maximize CT interactions.

3. RELATION BETWEEN OPTICAL AND THERMAL ELECTRON TRANSFER

We have shown recently that in solution d^{10} and d^8 complexes[18–21,29] exhibit weak IPCT bands (ϵ = 40 $M^{-1}cm^{-1}$ for $PQ[Pt(mnt)_2]$[19]) in the region of 400–1200 nm. When for the nickel and platinum complexes the acceptor is varied from PQ^{2+} to BQ^{2+} and MQ^{2+}, the maxima of these bands are shifted to higher energy

according to the Hush relation,[30a] $E_{op} = \chi + \Delta G_{IP}$, wherein E_{op} is obtained from the maximum of the IPCT band and ΔG_{IP}, the driving force of electron transfer within the contact ion pair, from the difference in the components redox potentials and the association constants of the ions before and after electron transfer. The total reorganization energy χ was obtained as 64 ± 5 and 47 ± 9 kJ·mol^{-1} for A[M(mnt)$_2$] and A[M(dmit)$_2$], respectively. The smaller value of the dmit-complexes as compared to the mnt-compounds may be due to their more extended π-system, in accord with the weaker solvent effect on the redox potentials.[19] When the ethene-bridged acceptor E–DPE–Me^{2+} is present in the above mentioned ion pairs, χ does not change significantly, while introduction[28a] of the tetrahedral dithiolene zincate increases χ to 115 kJ·mol^{-1}.

The free activation enthalpy of thermal electron transfer (ΔG^*) is the range of 130–170 kJ·mol^{-1} as calculated from E_{op} and ΔG_{IP} according to $\Delta G^* = E_{op}^2/4(E_{op} - \Delta G_{IP})$.[30b] From these values approximate potential energy curves can be constructed as shown in Fig. 5. As can be seen from the location of the upper curves, the back-electron transfer reaction is located at the beginning of the "Marcus inverted region."

The extent of charge delocalization between $[ML_2]^{2-}$ and A^{2+} is described by the parameter α^2 which is directly proportional to the integrated intensity of the IPCT band and indirectly propor-

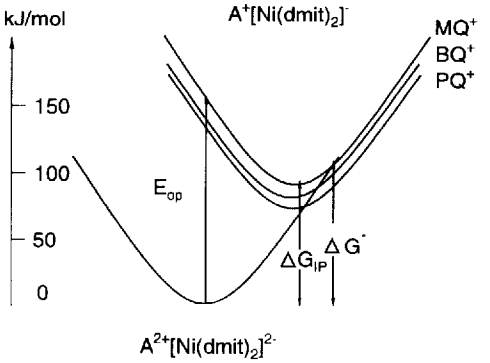

FIGURE 5 Potential energy curves for electron transfer within A[Ni(dmit)$_2$] in DMSO/THF = 1/1 (v/v) as obtained from E_{op} and ΔG_{IP}.

tional to E_{op} and the square of the inter-reactant distance between the two ions.[30,31] Taking the latter as 560 pm one obtains a value of 2.2×10^{-4} for $PQ[Pt(mnt)_2]$.[19] This is almost identical to the value reported[31] for $MV^{2+}/[Fe(CN)_6]^{4-}$ and indicates a very small amount of delocalization which is typical for outer-sphere complexes.[32,33] Correspondingly, the electronic coupling between the two redox states is rather weak as indicated by the values of 220 and 200 cm^{-1} (2.7 and 2.4 $kJ \cdot mol^{-1}$), obtained for the electron exchange matrix element H_{DA} from the relation $H_{DA} = E_{op} \times \alpha$. The corresponding splitting of the two curves at the intersection point[30,31] is given by $2H_{DA}$ but is omitted for the purpose of simplicity in Figs. 5 and 8.

Due to the low absorptivity of the IPCT band and its overlap with dithiolene metallate absorptions it is often difficult to locate the maximum from solution data with satisfying accuracy and reproducibility. This difficulty is overcome when the onset of the band in the Diffuse Reflectance Spectra of the powder is taken as the energy of the IPCT transition (E_{IPCT}).[34] As compared to E_{op}, obtained from the maximum in solution, the E_{IPCT} values are smaller by 20 to 50 $kJ \cdot mol^{-1}$. Figure 6 illustrates the spectral changes when in $(NBu_4)_2[Ni(dmit)_2]$ the cations are replaced by OV^{2+} and BQ^{2+}. The low-energy absorption of the tetrabutylammonium salt (Fig. 6, spectrum A) at 1050 and 1250 nm has not been recognized previously. It is assigned to a new type of ligand-centered transition between occupied and empty molecular orbitals localized at both entire ligands and both peripheral CS_3-fragments, respectively.[36]

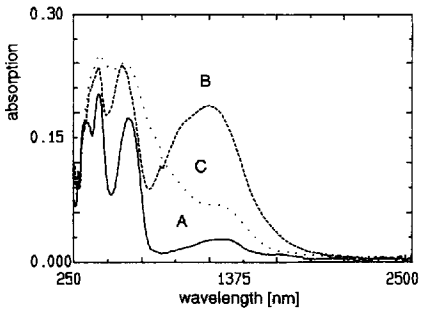

FIGURE 6 Diffuse Reflectance Spectra of $(NBu_4)_2[Ni(dmit)_2]$ (spectrum A), $OV[Ni(dmit)_2]$ (spectrum B) and $BQ[Ni(dmit)_2]$ (spectrum C).

A coplanar arrangement of the two ligands is necessary to allow this interaction since no corresponding bands are observable in the tetrahedral zinc complexes. Introduction of OV^{2+} induces the appearance of a broad IPCT band at about the same wavelength (spectrum B), while in the case of the poorer acceptor BQ^{2+} the band is shifted to higher energy (spectrum C). The corresponding onset wavelengths are 1453 and 984 nm, respectively.

As for E_{op} obtained from solution data, the E_{IPCT} values also follow a modified Hush relation:

$$E_{IPCT} = \chi + \Delta G_{12}. \tag{1}$$

Since in the solid state there exists no association equilibrium, ΔG_{12} which is directly obtainable from the redox potential difference $E(A^{2+/+}) - E([ML_2]^{-/2-})$, is used instead of ΔG_{IP}. Note that ΔG_{12} is the driving force for electron transfer between the fully solvated free ions in solution:

$$A^{2+} + [ML_2]^{2-} = A^{+} + [ML_2]^{-}. \tag{2}$$

From a corresponding plot for thirty-two complexes a linear regression analysis reveals a slope of 0.9 and a reorganization energy of 60 $kJ \cdot mol^{-1}$ (Fig. 7). The deviation from the theoretical slope of 1.0 is not surprising since it is unlikely that the intrinsic barriers of electron transfer are the same for all compounds.

As discussed for the solution data, potential energy curves can be constructed from the E_{IPCT}, ΔG_{12}, and ΔG^* values which are summarized in Table I. Figure 8 shows that the system $MV[M(dmit)_2]$ is not in the "inverted region" and that the activation energy of back-electron transfer is smaller for M = Pd (2–6 $kJ \cdot mol^{-1}$) than for Pt and Ni (3–10 $kJ \cdot mol^{-1}$). In agreement with this observation the values of H_{AD} are generally larger for M = Pd than for M = Ni, Pt as demonstrated by the values of 360 and 299 cm^{-1} calculated for $MV[Pd(dmit)_2]$ and $MV[Ni(dmit)_2]$, respectively.[36] This suggests a stronger coupling of the two surfaces at the intersection point and therefore a lower barrier to back-electron transfer in the case of the palladium ion pairs. A plot of ΔG^* as a function of ΔG_{12} for twenty-five complexes reveals that the free activation enthalpy decreases linearly with increasing driving force.

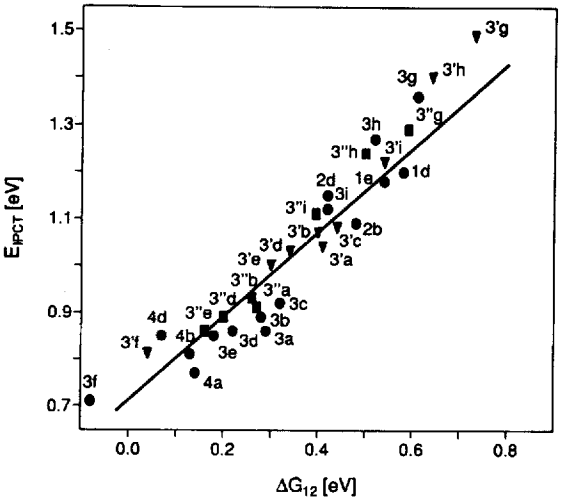

FIGURE 7 Dependence of the onset of the IPCT band, obtained from Diffuse Reflectance Spectra, on ΔG_{12}, the driving force of electron transfer between the solvent separated ions in solution. ●, ▼, ■ correspond to Ni, Pd and Pt complexes, respectively.

Copper complexes have not been included in the plot according to Fig. 7 since they may have a tetrahedral geometry as was reported for the similar ion pair (1-ethylpyridinium)$_2$[Cu(dmit)$_2$].[37]

In summary we can state that for a large number of d^8 complex ion pairs the reorganization energy of electron transfer stays approximately constant and the free activation enthalpy decreases linearly when the driving force is increased from $+0.7$ to -0.1 eV.

4. ELECTRICAL DARK- AND PHOTOCONDUCTIVITY

Electrical Dark Conductivity

While zinc compounds have specific conductivities lower than 10^{-12} $\Omega^{-1}cm^{-1}$, the values of the other complexes are in the range of 10^{-10} to 10^{-3} $\Omega^{-1}cm^{-1}$. From the variations of electrical parameters of pressed powder pellets with the driving force ΔG_{12} (Eq. (2), Table I) two types of complexes can be distinguished. For Class I compounds which contain Ni, Pd or Pt and one of the good

TABLE I

Redox potentials of solvent separated ions, free reaction (ΔG_{12}) and activation (ΔG^*) enthalpies of electron transfer between the ions, and electrical parameters (log σ, E_a) and onset of IPCT band (E_{IPCT}) of solid ion pairs.

Compound	Nr.	$E(D^{-/2-})$[a]	$E(A^{2+/+})$	ΔG_{12}[b]	log σ[c]	E_a[d]	ΔG^*[d]	E_{IPCT}[d]
MQ[Ni(dmit)$_2$]	**3g**	−0.14	−0.75	+0.61	−5.57	0.33	0.61	1.36
MQ[Pd(dmit)$_2$]	**3′g**	−0.02	−0.75	+0.73	−6.32	0.29	0.73	1.51
MQ[Pt(dmit)$_2$]	**3″g**	−0.16	−0.75	+0.59	−4.60	1.29		
BQ[Ni(dmit)$_2$]	**3h**	−0.14	−0.66	+0.52	−6.15	0.42		1.27
BQ[Pd(dmit)$_2$]	**3′h**	−0.02	−0.66	+0.64	−6.39	0.26	0.64	1.40
BQ[Pt(dmit)$_2$]	**3″h**	−0.16	−0.66	+0.50	−4.04			1.24
PQ[Ni(dmit)$_2$]	**3i**	−0.14	−0.56	+0.42	−5.39	0.35	0.45	1.12
PQ[Pd(dmit)$_2$]	**3′i**	−0.02	−0.56	+0.54	−6.26	0.28	0.55	1.22
PQ[Pt(dmit)$_2$]	**3″i**	−0.16	−0.56	+0.40	−3.89		0.43	1.11
StV[Ni(dmit)$_2$]	**3c**	−0.14	−0.46	+0.32	−6.60		0.35	0.92
StV[Pd(dmit)$_2$]	**3′c**	−0.02	−0.46	+0.44	−10.09	0.75	0.46	1.08
StV[Pt(dmit)$_2$]	**3″c**	−0.16	−0.46	+0.30	−7.59	0.45	0.32	0.83
MV[Ni(dmit)$_2$]	**3a**	−0.14	−0.43	+0.29	−5.92	0.26	0.32	0.86
MV[Pd(dmit)$_2$]	**3′a**	−0.02	−0.43	+0.41	−6.96	0.39	0.43	1.04
MV[Pt(dmit)$_2$]	**3″a**	−0.16	−0.43	+0.27	−5.60	0.31	0.32	0.91
OV[Ni(dmit)$_2$]	**3b**	−0.14	−0.42	+0.28	−6.85	0.54	0.32	0.89
OV[Pd(dmit)$_2$]	**3′b**	−0.02	−0.42	+0.40	−9.00	0.59	0.43	1.07
OV[Pt(dmit)$_2$]	**3″b**	−0.16	−0.42	+0.26	−7.54	0.51	0.32	0.93
DQ[Ni(dmit)$_2$]	**3d**	−0.14	−0.36	+0.22	−6.02	0.46	0.29	0.86
DQ[Pd(dmit)$_2$]	**3′d**	−0.02	−0.36	+0.34	−6.42	0.32	0.38	1.03
DQ[Pt(dmit)$_2$]	**3″d**	−0.16	−0.36	+0.20	−5.72	0.27	0.29	0.89
DP[Ni(dmit)$_2$]	**3e**	−0.14	−0.32	+0.18	−5.37	0.34	0.27	0.85
DP[Pd(dmit)$_2$]	**3′e**	−0.02	−0.32	+0.30	−5.80	0.27	0.36	1.00
DP[Pt(dmit)$_2$]	**3″e**	−0.16	−0.32	+0.16	−4.77	0.25	0.26	0.86

DPK[Ni(dmit)$_2$]	**3f**	−0.14	−0.06	−0.08	−3.50	0.15	0.16	0.71
DPK[Pd(dmit)$_2$]	**3'f**	−0.02	−0.06	+0.04	−5.40	0.17	0.21	0.81
StV[Ni(dmid)$_2$]	**4c**	−0.29	−0.46	+0.17	−7.81		0.24	0.77
MV[Ni(dmid)$_2$]	**4a**	−0.29	−0.43	+0.14	−5.55	0.34	0.24	0.77
OV[Ni(dmid)$_2$]	**4b**	−0.29	−0.42	+0.13	−4.80	0.31	0.24	0.81
DQ[Ni(dmid)$_2$]	**4d**	−0.29	−0.36	+0.07	−5.98	0.24	0.23	0.85
DQ[Ni(mnt)$_2$]	**1d**	+0.22	−0.36	+0.58	−10.90	0.58	0.58	1.20
DP[Ni(mnt)$_2$]	**1e**	+0.22	−0.32	+0.54	−8.28	0.57	0.54	1.18
OV]Ni(dmt)$_2$]	**2b**	+0.06	−0.42	+0.48	−8.34	0.49	0.49	1.09
DQ[Ni(dmt)$_2$]	**2d**	+0.06	−0.36	+0.42	−7.64	0.35	0.45	1.15
MQ[Cu(dmit)$_2$]	**3*g**	−0.02	−0.75	+0.73	<-11.00		0.77	1.35
BQ[Cu(dmit)$_2$]	**3*h**	−0.02	−0.66	+0.64	−7.52		0.64	1.35
PQ[Cu(dmit)$_2$]	**3*i**	−0.02	−0.56	+0.54	−8.19		0.55	1.28
DP[Cu(dmit)$_2$]	**3*e**	−0.02	−0.32	+0.30	−8.53	1.44	0.30	0.67
DPK[Cu(dmit)$_2$]	**3*f**	−0.02	−0.06	+0.04	−7.97	1.29	0.19	0.73

[a]From cyclic voltammetry in MeCN, [V] vs. SCE.
[b][eV].
[c][Ω^{-1}cm^{-1}].
[d][eV].

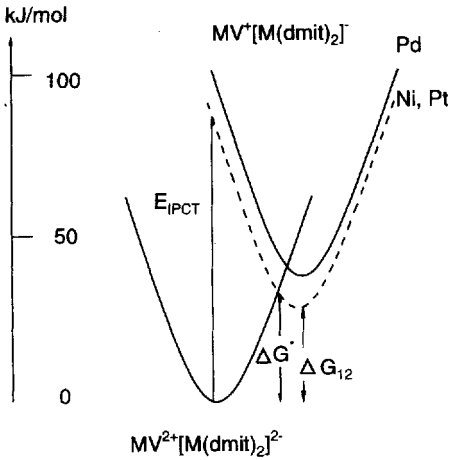

FIGURE 8 Potential energy curves for electron transfer in the system MV[M(dmit)$_2$] as obtained from E_{IPCT} and ΔG_{12}.

acceptors **a**–**f** ($E^{2+/+} = -0.42$ to -0.06 V) the electrical conductivity increases with larger driving force. Contrary to that, σ does not change significantly for Class II complexes which all have one of the poorer acceptors **g**–**i** ($E^{2+/+} = -0.75$ to -0.56 V) or Cu as the central metal. For both classes the temperature dependence of σ, measured in the range of 20 to 110°C, follows a typical Arrhenius relation, and activation energies E_a were obtained from the plots of log σ vs. $1/T$ which in all cases exhibited excellent linearity.

When log σ is plotted as function of E_a, an approximately linear relationship is found for both classes of compounds (Fig. 9). This indicates that changes in σ originate only in changes[38] of E_a according to the equation log σ = const. $-bE_a$. In order to test how the conductivity depends on ΔG_{12}, which can be taken as a measure for the amount of charge transferred, in a regular fashion, the log σ values of all thirty-two complexes are plotted as functions of decreasing driving force in Fig. 10. As can been recognized, only the twenty-three Class I compounds exhibit a linear increase with more negative ΔG_{12} while the remaining nine Class II complexes are influenced only negligibly. Thus, for ion pairs with planar acceptors the conductivity can be quantitatively predicted from the components redox potentials. It is likely that Class I complexes all

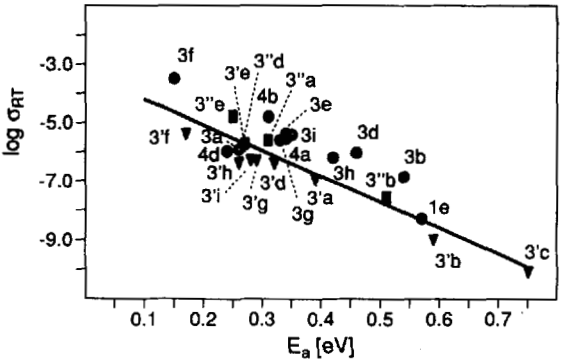

FIGURE 9 Dependence of the specific electrical conductivity, plotted as log σ ($\Omega^{-1}cm^{-1}$), of pressed powder pellets on the activation energy.

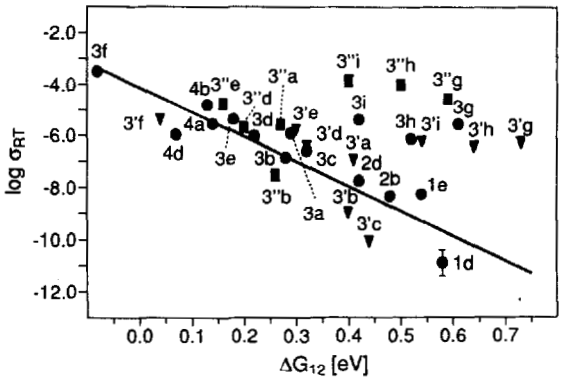

FIGURE 10 Dependence of log σ ($\Omega^{-1}cm^{-1}$) of pressed powder pellets on ΔG_{12}.

form mixed donor–acceptor stacks as indicated by the X-ray results for the mnt-complexes. This arrangement allows a maximized CT interaction, while that is not the case for Class II compounds as indicated by the structure of BQ[Ni(mnt)$_2$].

These results suggest that the activation energy of the electrical dark conductivity of Class I complexes is largely determined by the degree of CT interaction within the ion pairs which should increase with decreasing free activation enthalpy ΔG^* of the electron transfer reaction (Eq. (2)). The latter is obtainable within the Hush–Marcus model from E_{IPCT} and ΔG_{12}, and the data are sum-

marized in Table I. From the approximately linear dependence of log σ on ΔG^* (Fig. 11) one can conclude that charge generation in the solid occurs by electron transfer from the dithiolene metallate donor to the bipyridinium acceptor. Since *ab initio* band calculations for $(NBu)_4[Ni(mnt)_2]$, $MV[Ni(mnt)_2]$ and $MV[Ni(dmit)_2]$ in no case indicate the presence of energy bands for these solids, it is suggested that charge migration occurs by a hopping mechanism.[39]

The influence of steric alteration in the acceptor on the electrical parameters was tested with the ethene-bridged viologen isomers E- and Z- DPE-Me^{2+} shown in Fig. 1. Since the trans-form is the better acceptor, as indicated by the reduction potential of -0.51 as compared to -0.61 V for the cis-isomer, one expects a higher conductivity for the ion pair of the former when steric influences would be negligible. It turns out[27] that in the case of DPE-$Me[Ni(mnt)_2]$ the electrical parameters are almost the same for both isomers while σ increases from 5×10^{-7} to 5×10^{-6} $\Omega^{-1}cm^{-1}$ when the trans-acceptor is replaced by the cis-isomer in DPE-$Me[Ni(dmit)_2]$. Thus, only the latter ion pair may change its electrical conductivity as a consequence of light-induced cis-trans isomerization. The control of a physical property through light absorption in a central topic of photonics, an important part of materials science.

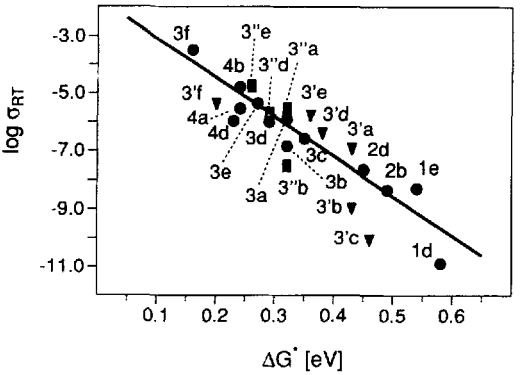

FIGURE 11 Dependence of log σ ($\Omega^{-1}cm^{-1}$) of pressed powder pellets of Class I complexes on the free activation enthalpy of electron transfer ΔG^* as calculated from ΔG_{12} and E_{IPCT}.

When the above conclusion is correct, that the first step in the conductivity mechanism is electron transfer, one expects that irradiation should have a pronounced effect since solution experiments have demonstrated that photoinduced electron transfer can take place.[40,41] In fact, when in $(NBu_4)_2[Ni(mnt)_2]$ the cation is replaced by the redoxactive MV^{2+}, the photoconductivity (λ = 696 nm) increases from $\leq 10^{-12}$ to $4 \times 10^{-9}\ \Omega^{-1}cm^{-1}$. In the case of the 1:2 ion pairs which do not have CT character, the corresponding changes are negligible as indicated by the values of 1×10^{-9} and $2 \times 10^{-9}\ \Omega^{-1}cm^{-1}$ when $NBu_4[Ni(mnt)_2]$ is compared with $MV[Ni(mnt)_2]_2$.[42-44]

Electrical Photoconductivity

Further evidence for the promoting effect of CT interaction stems from the wavelength dependence of photoconductivity and from photovoltage measurements. In order to prevent interference by metal centered states, the zinc complexes $\{A^{2+}[Zn(mnt)_2]^{2-}\}$ were examined. Surprisingly, the photoconductivity has a maximum in the region of the IPCT band. Such behavior has been predicted for intervalence complexes[30a] and again supports the validity of the Hush model for these redoxactive ion pairs. In the sequence A^{2+} = DQ^{2+}, PQ^{2+}, BQ^{2+}, the photoconductivity maxima are located at 760, 600 and 570 nm and their wavenumbers increase linearly with more negative potential of the acceptor.[43,44] In the optical spectra the corresponding IPCT maxima are shifted by about 60 nm to the blue. A similar shift was observed for CT complexes between tetranitrofluorenone and dibenzothiophene.[45]

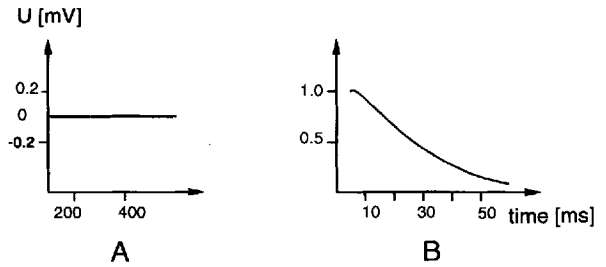

FIGURE 12 Decay of Dember Voltage obtained upon laser excitation (337 nm) of pressed powder pellets of $(NBu_4)_2[Zn(mnt)_2]$ (A) and $PQ[Zn(mnt)_2]$ (B).

Measurement of the time resolved photovoltage (Dember Spectrum) of pressed powder pellets is successful only when a redox-active cation is present as shown in Fig. 12 for $(NBu_4)_2[(Zn(mnt)_2]$ and $PQ[Zn(mnt)_2]$. Laser excitation at a wavelength of 337 nm affords a transient voltage with a half-life of 20 milliseconds.[46] The same result is obtained with the corresponding nickel mnt- and dmit-complexes. This clearly demonstrates that only solids of CT character are able to generate surface charges upon light absorption.

5. SUMMARY

The results summarized in this review demonstrate that ion pairs consisting of doubly-charged planar and reversible redox systems are excellent candidates to control the electrical conductivity of the solid material by modifying the free activation enthalpy ΔG^* of electron transfer. The latter is easily obtainable from the energy of the IPCT band and the components redox potentials through application of the Hush–Marcus model. It is found that the logarithm of electrical conductivity increases linearly with decreasing ΔG^*. Although the electronic interaction within the ion pairs is small, the conductivity increases by seven orders of magnitude when ΔG^* decreases from 0.73 to 0.15 eV. This holds only for complexes (Class I) whose structure consists of an alternating donor–acceptor stack of planar components but not for ion pairs (Class II) having a non-planar acceptor. In the latter case changes in ΔG^* do not significantly affect the conductivity. By the use of a photoisomerizable acceptor it is found that *trans* to *cis* isomerization increases the conductivity by one order of magnitude. Such a type of system may be suited to modulating this important physical property through light absorption, a phenomenon of central interest to the area of photonics. It is proposed that charge generation in Class I complexes occurs by electron transfer while charge migration takes place by a hopping mechanism. In accord with this proposal is the observation that the electrical photoconductivity is much larger for ion pairs of CT character and that its wavelength dependence has a maximum in the region of the IPCT band. In

complete analogy to the latter, the maximum can be shifted in a predictable manner by variation of the molecular redox potentials.

Acknowledgments

This work was supported by Deutsche Forschungsgemeinschaft and Fonds der Chemischen Industrie. Helpful cooperation with Prof. Dr. H. Meier, Bamberg, and Doz.-Dr. G. Israel, Merseburg, is gratefully acknowledged.

References

1. P. N. Prasad and D. J. Williams, *Introduction to Nonlinear Optical Effects in Molecules and Polymers* (J. Wiley and Sons, 1991).
2. (a) R. C. Wheland, J. Am. Chem. Soc. **98**, 3926 (1976). (b) R. C. Wheland and J. L. Gillson, *ibid.* p. 3916.
3. P. Cassoux, L. Valade, H. Kobayashi, A. Kobayashi, R. A. Clark and A. E. Underhill, Coord. Chem. Rev. **110**, 115 (1991).
4. D. R. Rosseinsky and R. E. Malpas, J. Chem. Soc. Dalton Trans. **1979**, 749.
5. D. R. Rosseinsky and R. E. Malpas, J. Chem. Commun. **1977**, 455.
6. J. S. Tonge and A. E. Underhill, J. Chem. Soc. Dalton Trans. **1984**, 2333.
7. G. J. Ashwell, G. H. Cross, D. A. Kennedy, I. W. Nowell and J. G. Allen, J. Chem. Soc. Perkin Trans. II **1983**, 1787.
8. E. J. Rosa and G. N. Schrauzer, J. Phys. Chem. **73**, 3132 (1969).
9. P. I. Clemenson, Coord. Chem. Rev. **106**, 171 (1990).
10. H. Kisch, Coord. Chem. Rev. **125**, 155 (1993).
11. B. Emmert and H. Lauritzen, Chem. Ber. **71**, 240 (1938).
12. A. J. MacFarlane and R. J. P. Williams, J. Chem. Soc. (A) **1969**, 1517.
13. C. K. Prout and P. Murray-Rust, J. Chem. Soc. (A) **1969**, 1520.
14. E. G. Meghee, C. E. Johnson and R. Eisenberg, Inorg. Chem. **28**, 2423 (1989).
15. K. B. Yoon and J. K. Kochi, J. Am. Chem. Soc. **111**, 1128 (1989).
16. B. L. Atwood, N. Spencer, H. Shariari-Zavareh, J. F. Stoddart and D. J. Williams, J. Chem. Soc. Chem. Commun. **1987**, 1064.
17. I. Willner, Y. Eichen, M. Rabinovitz, R. Hoffman and Sh. Cohen, J. Am. Chem. Soc. **114**, 637 (1992).
18. S. Lahner, Y. Wakatsuki and H. Kisch, Chem. Ber. **120**, 1011 (1987).
19. W. Dümler and H. Kisch, Nouv. J. Chem. **15**, 649 (1991).
20. H. Kisch, F. Nüsslein and I. Zenn, Z. Anorgan. Allg. Chem. **600**, 67 (1991).
21. H. Kisch, A. Fernandez, Y. Wakatsuki and H. Yamazaki, Z. Naturforsch. **40b**, 292 (1985).
22. Ch. A. Hunter and J. K. M. Sanders, J. Am. Chem. Soc. **112**, 5525 (1990).
23. C. K. Prout and J. D. Wright, Angew. Chem. **80**, 688 (1968); Angew. Chem. Int. Ed. Engl. **20**, 695 (1968).
24. J. Burdon, M. H. B. Hayes and M. E. Pick, J. Environ. Sci. Health Section **B12**, 37 (1977).
25. M. Lemke, F. Knoch and H. Kisch, Acta Crystallogr. **C49**, 1630 (1993).
26. J. A. McCleverty, Progr. Inorg. Chem. **10**, 49 (1968).

27. G. Schmauch, F. Knoch and H. Kisch, Chem. Ber., **127**, 287 (1994).
28. (a) G. Schmauch, F. Knoch and H. Kisch, unpublished. (b) MV^{2+} is also planar in the halogenometallates (Ref. 13); *Ab initio* calculations indicate that this configuration is only 19 $kJ \cdot mol^{-1}$ above the lowest-energy geometry which has a twist angle of 60°: H. Wolkers, R. Stegmann, G. Frenking, K. Dehnicke, D. Fenske and G. Baum, Z. Naturforsch. **48b**, 1341 (1993).
29. F. Nüsslein, R. Peter and H. Kisch, Chem. Ber. **122**, 1023 (1989).
30. (a) N. S. Hush, Progr. Inorg. Chem. **8**, 391 (1967). (b) R. A. Marcus and N. Sutin, Comments Inorg. Chem. **5**, 119 (1986).
31. J. L. Curtis, B. P. Sullivan and T. J. Meyer, Inorg. Chem. **19**, 3833 (1980).
32. T. J. Meyer, Acc. Chem. Res. **11**, 94 (1978).
33. H. Taube, Ann. N. Y. Acad. Sci. **313**, 481, 496 (1978).
34. To avoid errors due to the slightly differing amounts of solid material employed, the extrapolation method according to Ref. 35 was used.
35. B. Karvaly and I. Hevesi, Z. Naturforsch. **26a**, 245 (1971).
36. I. Nunn, B. Eisen, R. Benedix, C. Nieke and H. Kisch, unpublished.
37. G. Matsubayashi, K. Takahashi and T. Tanaka, J. Chem. Soc. Dalton Trans. **1988**, 967.
38. K. Ulbert, J. Polymer. Sci. C **22**, 881 (1969).
39. G. Schmauch, P. Otto and H. Kisch, unpublished.
40. A. Fernandez and H. Kisch, Chem. Ber. **117**, 3102 (1984).
41. H. Kisch, W. Dümler, C. Chiorboli, F. Scandola, J. Salbeck and J. Daub, J. Phys. Chem. **96**, 10323 (1992).
42. H. Meier, W. Albrecht, H. Kisch and F. Nüsslein, J. Phys. Chem. **93**, 7726 (1989).
43. H. Meier, W. Albrecht, H. Kisch, I. Nunn and F. Nüsslein, Synthetic Metals **48**, 111 (1992).
44. H. Meier, W. Albrecht and H. Kisch, Mol. Cryst. Liq. Cryst. **217**, 153 (1992).
45. T. K. Mukerjee, J. Phys. Chem. **74**, 3006 (1970).
46. G. Israel und H. Kisch, unpublished.